

High Resolution Imaging of Normal and Osteoarthritic Cartilage with Optical Coherence Tomography

JURGEN M. HERRMANN, COSTAS PITRIS, BRETT E. BOUMA, STEPHEN A. BOPPART, CHRISTINE A. JESSER, DEBRA L. STAMPER, JAMES G. FUJIMOTO, and MARK E. BREZINSKI

ABSTRACT. Objective. We describe optical coherence tomography (OCT), a high resolution micron scale imaging technology, for assessment of osteoarthritic articular cartilage microstructure. OCT is analogous to ultrasound, measuring the intensity of backreflected infrared light rather than acoustical waves.

Methods. OCT imaging was performed on over 100 sites on 20 normal and osteoarthritic cartilage specimens *in vitro*.

Results. Microstructures that were identified included fibrillations, fibrosis, cartilage thickness, and new bone growth at resolutions between 5 and 15 μm . In addition, the polarization sensitivity of imaging suggested a diagnostic role of polarization spectroscopy.

Conclusion. OCT represents an attractive new technology for intraarticular imaging due to its high resolution (greater than any available clinical technology), ability to be integrated into small arthroscopes, compact portable design, and relatively low cost. (J Rheumatol 1999;26:627-35)

Key Indexing Terms:

OPTICAL COHERENCE TOMOGRAPHY OSTEOARTHRITIS CARTILAGE
ARTHROSCOPY SYNOVIAL BIOPSY BIOMEDICAL IMAGING

Osteoarthritis (OA) or degenerative joint disease affects an estimated 40 million persons in the USA. Although all tissues within the osteoarthritic joint show morphologic changes, the hallmark of OA is the degeneration of cartilage. Many investigators have shown that the progression of articular damage may be modified at early stages either by medical or surgical intervention¹⁻³. This has resulted in a need for methods of detecting degenerative cartilage abnormalities early in their progression, when intervention is likely to have its greatest effect. Early markers of joint degradation that precede reductions in the joint space (as seen with radiography) range from microstructural abnormalities such

as cartilage thinning, changes in chondrocyte concentrations, and fibrillations to biochemical abnormalities such as changes in the concentration of water, glycosaminoglycans, and collagen⁴.

A variety of imaging modalities have been applied to the assessment of early cartilage abnormalities, including conventional radiography, ultrasound, computed tomography (CT), magnetic resonance imaging (MRI), and arthroscopy, with limited results⁴⁻¹⁰. Conventional radiography, CT, and conventional ultrasound, although powerful technologies for a wide range of clinical scenarios, have axial resolutions in excess of 500 μm , which is insufficient for the identification of most microstructural changes⁵⁻⁷. High frequency ultrasound transducers (25 MHz) can increase axial resolution to 0.1 mm, but their limitations include an inability to image near the cellular level, a requirement for the presence of a transducing medium, the relatively large transducer size, and the limited penetration (few millimeters)⁸. Needle arthroscopy provides a direct, magnified view of the articular surfaces of the joint as well as other supportive structures such as the menisci⁹. However, direct visualization does not allow imaging below the tissue surface, severely limiting the amount of diagnostic information that can be attained.

MRI represents a powerful tool for evaluating joint abnormalities, particularly when using a surface coil^{10,11}. Although even high performance clinical systems cannot generate resolutions better than 100 μm , MRI has had some success in identifying cartilage softening and swelling, in part because of its ability to monitor biochemical as well as structural changes. However, difficulties with MRI include its high cost, especially if serial screening is required, and the time necessary for data acquisition. Furthermore, because of the low axial resolution, it has yet to be shown

From the Department of Electrical Engineering and Computer Science and the Research Laboratory of Electronics, Massachusetts Institute of Technology, Cambridge, MA; the Department of Biology, King's College, Wilkes-Barre, PA; and the Department of Medicine, Harvard Medical School, Boston, MA, USA.

Supported in part by National Institutes of Health contracts NIH-RO1-AR44812-01 (MEB), NIH-9-RO1-CA75289-01 (JGF), NIH-9-RO1-EY11289-10 (JGF), and NIH-1-R29-HL55686-01A1 (MEB), the Medical Free Electron Laser Program, Office of Naval Research Contract N00014-94-1-0717 (JGF), the Whitaker Foundation Contract 96-0205 (MEB), the National Institutes of Health and Deutsche Forschungsgemeinschaft Contract He2747/1-1.

J.M. Herrmann, PhD, Visiting Scientist; C. Pitris, MS, Graduate Student; B.E. Bouma, PhD, Postdoctoral Associate; S.A. Boppert, PhD, Graduate Student; J.G. Fujimoto, PhD, Professor, Department of Electrical Engineering and Computer Science and Research Laboratory of Electronics, Massachusetts Institute of Technology; D.L. Stamper, PhD, Assistant Professor, Department of Biology, King's College; C.A. Jesser, BS, Research Assistant; M.E. Brezinski, MD, PhD, Assistant Professor, Department of Medicine, Harvard Medical School.

Address reprint requests to Dr. M.E. Brezinski, Research Laboratory of Electronics, Massachusetts Institute of Technology, Building 36-357, 77 Massachusetts Ave., Cambridge, MA 02139. E-mail: mebrezin@mit.edu

Submitted September 29, 1997 revision accepted August 19, 1998.

that cartilage thickness can be measured with sufficient precision to monitor the effects of ongoing therapy.

Optical coherence tomography (OCT), a new method of micron scale imaging, has the potential of overcoming limitations of current imaging methods¹². OCT is analogous to B mode ultrasound, measuring the intensity of backreflected infrared light rather than acoustical waves. The typical axial resolution of the OCT system is 5-15 μm . This is almost 10 times greater than the resolution of CT, ultrasound, or MRI. Furthermore, resolutions in the range of $< 5 \mu\text{m}$ have been achieved with the use of broad bandwidth lasers¹³. OCT was originally developed to image the transparent tissue of the eye with unprecedented resolution. Clinical studies are in progress evaluating its potential for a wide range of retinal macular diseases¹⁴. Recently, the identification of pathology has been achieved in nontransparent tissue, in part through the use of longer wavelengths in the near infrared¹⁵⁻¹⁷. However, because of the multiple scattering of light that occurs in nontransparent tissue, the imaging penetration is limited to roughly 4 mm. In essence, imaging is being performed at high resolution over about the same length as an excisional biopsy. For this reason, an OCT image is often described as an optical biopsy.

Several features make OCT attractive for intraarticular imaging in addition to its high resolution. First, OCT is optical fiber based, allowing easy integration with arthroscopes of relatively small diameter. Second, OCT is compact and portable, well suited for the outpatient setting. Third, OCT is noncontact, allowing imaging to be performed through air or transparent medium such as saline. Fourth, OCT imaging can be performed at high speeds, allowing information near the cellular level to be obtained from throughout the joint. Finally, because OCT is optically based, it can potentially be combined with absorption or polarization spectroscopy, allowing biochemical as well as structural information to be obtained from tissue.

We present imaging of normal and osteoarthritic cartilage performed with OCT *in vitro*, demonstrating its ultrahigh resolution.

MATERIALS AND METHODS

Articular cartilage was obtained from either postmortem examinations or postsurgical limb resections. Over 100 sites from 10 patients were examined, including the knee, hip, ankle, metatarsal, interphalangeal, elbow, intervertebral, and clavicular joints. The samples were stored in 0.9% saline with 0.1% sodium azide at 0°C. Imaging was performed on segments smaller than $10 \times 10 \text{ cm}$. The saline does not require degassing. Samples are selected based on their macroscopic appearance. The samples were placed on a translation stage, which permits the acquisition of multiple depth scans resulting in a 2 dimensional cross sectional image. For imaging, the cartilage surface is exposed to the light beam. The position of the invisible infrared light beam on the sample is monitored with a visible light guiding beam. The peripheral areas of the imaged sections are marked with microinjections of dye to permit comparison of the OCT images with histologic images. The histologic processing of the sample includes fixing in 10% formalin for 12 h and decalcifying for 24-48 h. Different microstructures were identified by staining with hematoxylin/eosin (H/E) and

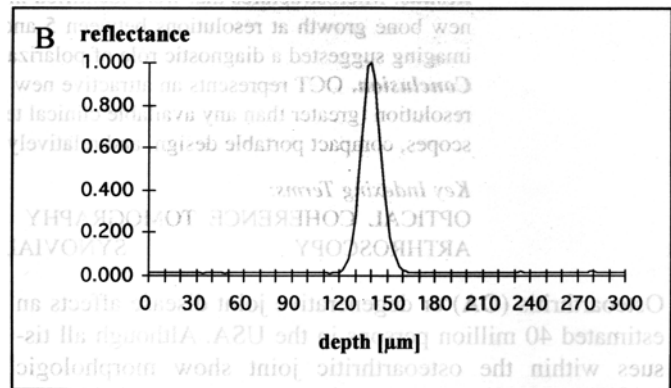
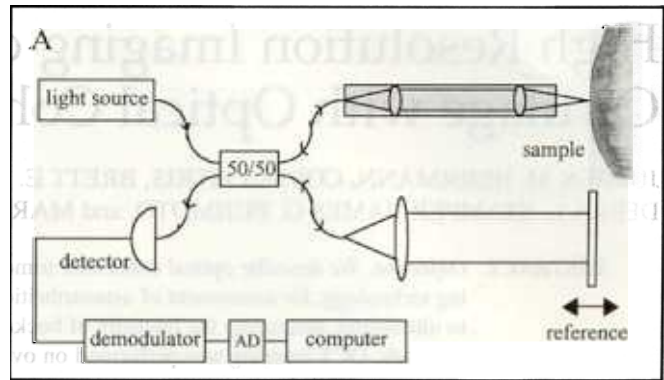


Figure 1. A. Schematic of the OCT system. B. A representative point spread function, which defines axial resolution.

trichrome blue. Stained histologic sections were compared with OCT images to allow correlation.

The principles behind OCT have been described¹². A schematic of the OCT system is shown in Figure 1. OCT measures the intensity of backreflected infrared light as a function of depth in a manner analogous to ultrasound. The time for light to return to the detector, or echo delay time, is used to measure distances. To produce cross sectional tomographic images the light beam is scanned across the tissue. The result is 2 or 3 dimensional data sets of the optical reflectance properties of the tissue.

Because of the high speed of light propagation, a direct measurement of the echo delay time cannot be made electronically. To measure the delay time (and optical path length) OCT uses a technique known as low coherence interferometry, which makes the system accurate and simple. The light is coupled into an optical fiber. The light is evenly split by an optical beam splitter. Half of the light is directed to a moving reference mirror and half is directed at the sample. The distance to the moving mirror is precisely controlled. Light reflected from structures within the tissue is combined with light reflected from the mirror. Interference occurs only if the path that light travels in both arms (optical pathlength) is almost identical. OCT measures the intensity of interference and uses this to represent the intensity of backreflection. The signal from the sample will only be measured if it has traveled the same distance as the controlled distance. By moving the mirror, the distance light travels in the reference arm is changed, which gives information from different depths within tissue.

A superluminescent diode light source (similar in some respects to sources used in compact disc players) or femtosecond solid state laser (generating pulses of 10^{-14} s duration) was used for imaging. The diode had a median wavelength of 1300 nm and a tunable spectral bandwidth of 50 nm, while the laser had a median wavelength of 1280 nm and a bandwidth of either 65 or 130 nm. The bandwidth $\Delta\lambda$ is essentially the wavelength dis-

tribution of the beam. The bandwidth is inversely related to the coherence length (which defines resolution) via the formula¹³

$$\Delta z = \frac{2 \ln 2}{\pi} \frac{\lambda^2}{\Delta \lambda}$$

The resolution of images was either 15, 11, or 5 μm , depending on the light source. The advantages of each source are outlined in the Discussion. The resolution was determined experimentally by measuring the axial point spread function using a mirror, a standard technique for defining resolution¹⁸. An example point spread function is shown in Figure 1B. The lateral resolution is determined by the spot size or focusing power of the lens system and was measured to be 10 μm . As with ultrasound, the axial and lateral resolution initially increase and then deteriorate as a function of depth in tissue. We measured the deterioration of resolution in tissue and it is (on average) a factor of 2 at 1.5 mm from the focus^{19,20}. Acquisition rates varied from 5 to 40 s, but systems have now been developed that can image at 4–8 frames/s. In addition, imaging at or near the video rate is likely with future technical advances. At the acquisition rate of current high speed sys-

tems, a square centimeter of articular surface 3 mm deep (300 pixels deep, 500 \times 50 pixels wide) would take 14 s.

In studies examining the effect of light polarization state on imaging, the polarization of the incident light was varied manually with fiber polarization controller paddles (Thor Labs, Newton, NJ, USA). Imaging at the same sites was performed with light whose polarization was switched to another polarization state.

To perform precision measurements of cartilage thickness, the refractive index of the tissue, a measure of the velocity of light in tissue, must be known. The refractive index of samples was measured for samples assessing cartilage thickness using described methods²¹. This method places sections of cartilage on a metal reflector and measures the apparent displacement of the reflector. The width of cartilage sections in an OCT image (Figure 2) were directly compared with histopathology. Cartilage thickness was determined at 3 sites on this patella at the center and \pm 1 mm from the center. At each site, 8 measurements were made 50–100 μm apart. Data represent means \pm the standard error.

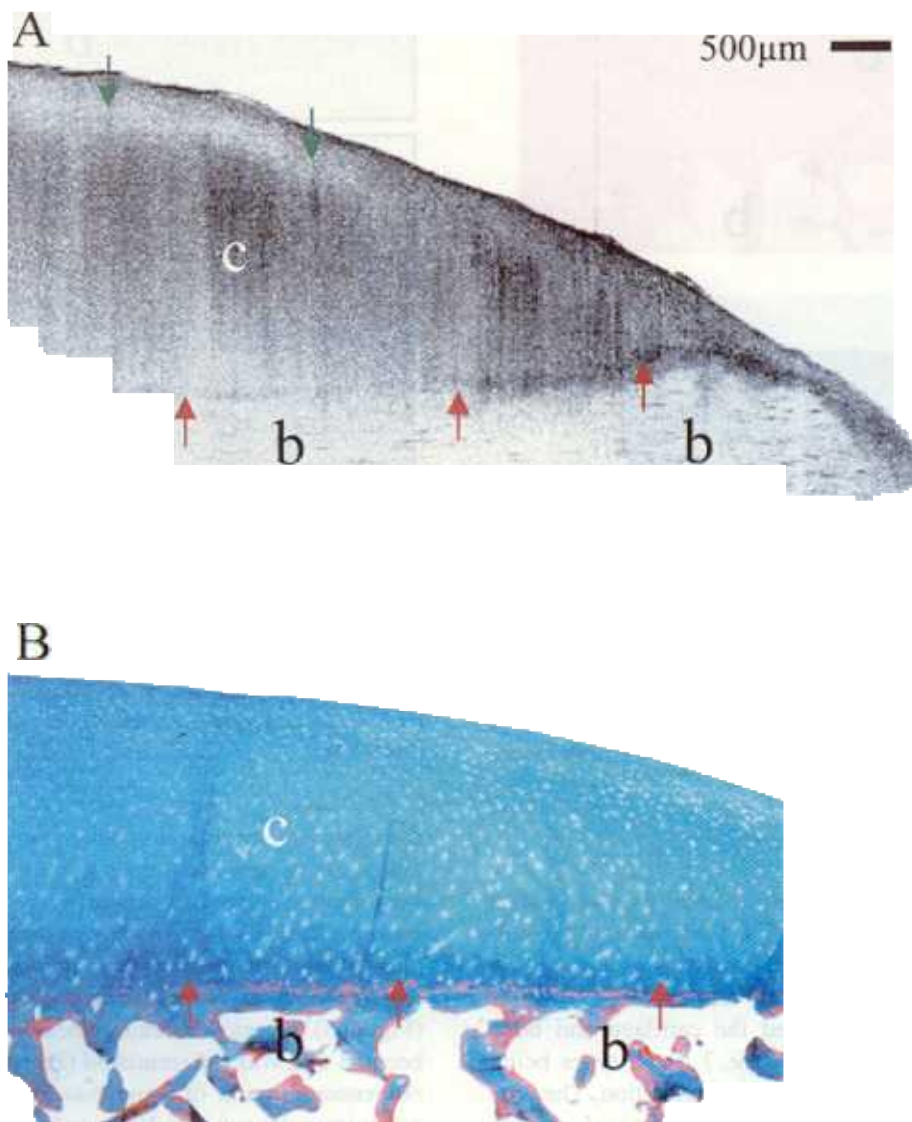


Figure 2. OCT image of the posterior surface of the patella (A) is compared with histology (B) (trichrome stain). The cartilage (c)-bone (b) interface (red arrows) is well defined. Green arrows show a region where the measured backreflected intensity is sensitive to the polarization state of the incident light. This is caused by the birefringence of the cartilage. The axial resolution (Δz) of this image is 5 μm .

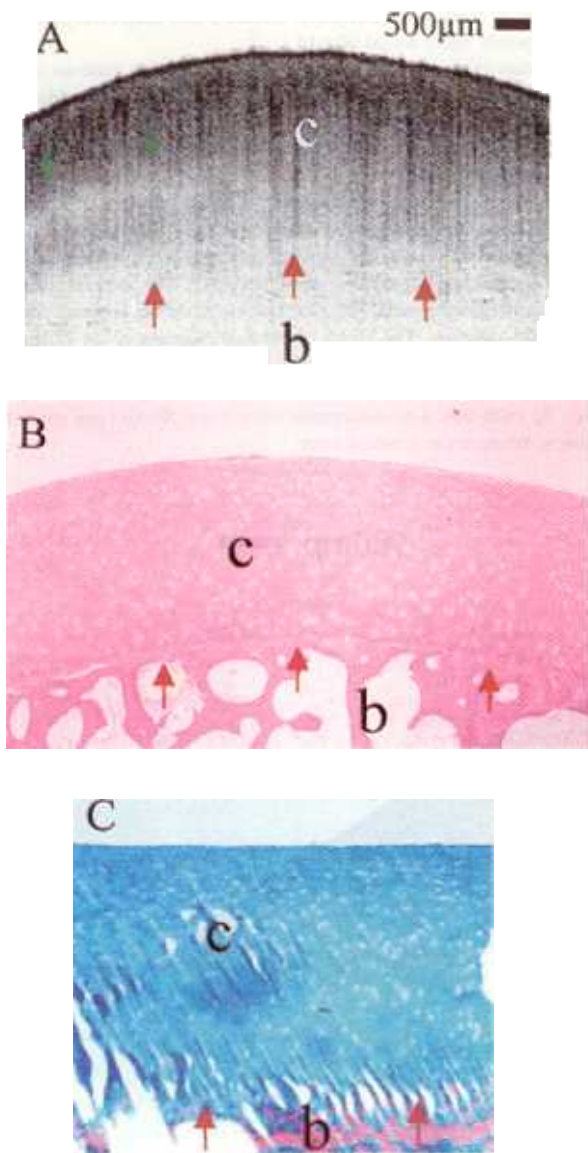


Figure 3. A. Cartilage (c) of the talus (Δz 11 μm). The corresponding histology is shown in B (H&E stain) and C (trichrome stain). Red arrows show the cartilage (c)-bone (b) interface, green arrows indicate a region of birefringence.

RESULTS

Cartilage with minimal osteoarthritic changes was imaged and is shown in Figures 2 through 4. Corresponding histology was performed and included. Emphasis was placed on viewing the contrast between bone and cartilage. Each of the OCT images sharply defined the cartilage and bone interface, the difference between the 2 tissue types being apparent in the varying degrees of backreflection. The posterior surface of the patella revealed cartilage of varying thickness (Figure 2).

The cartilage-bone interface of the talus was seen over 1.5 mm into the sample (Figure 3). A section of cartilage at

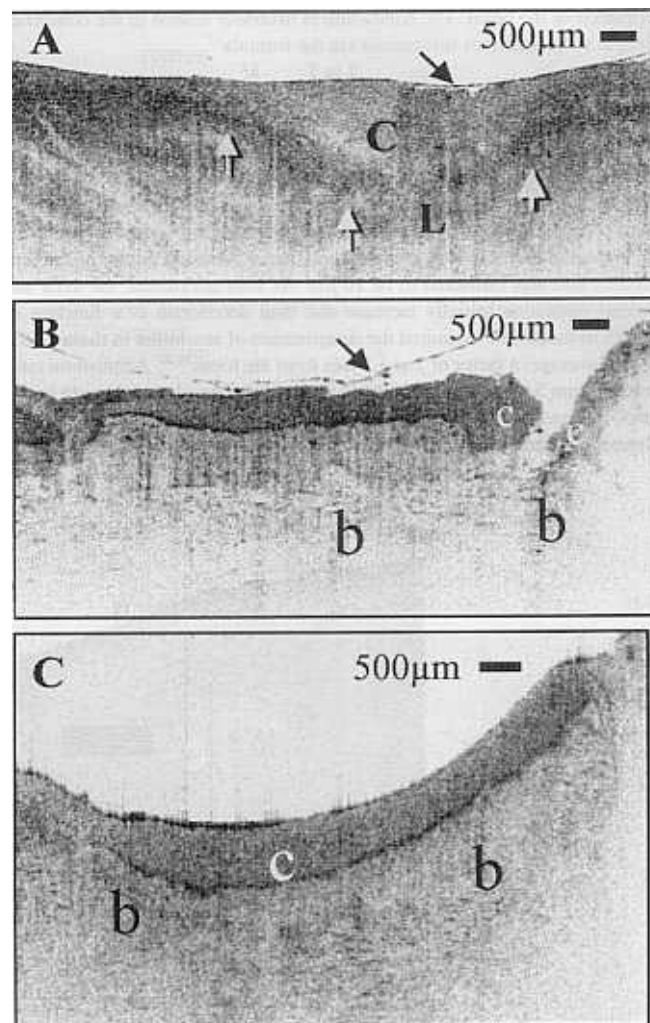


Figure 4. OCT images of an interphalangeal joint of the second toe. A. A section of cartilage is seen at the outer edge of the joint at the site of the ligament insertion (Δz 11 μm). An interface of cartilage and planes of fibrous tissue is indicated by arrows. B. Proximal (Δz 15 μm) and C. distal (Δz 11 μm) surfaces of the interphalangeal joints are shown. Cartilage (c)-bone (b) interfaces are defined sharply. The saline solution, visible as a narrow line above the cartilage (arrows, A and B), was applied to prevent the tissue from drying.

the outer edge of the interphalangeal joint at the site of ligament attachment was imaged and clear differentiation of the proximal and distal surfaces of the interphalangeal joints was seen (Figure 4). A medial meniscus overlying the articular cartilage of the knee was also imaged. Surface abnormalities were seen in the cartilage through the meniscus (Figure 5). A region of femoral head where the cartilage had become thin was differentiated (Figure 6). A large and heterogeneous region of bone was also seen that represents either irregular subchondral bone or new bone formation. A fibrous layer was noted at the surface of the cartilage. The sternoclavicular joint cartilage had become fibrocartilage and a mosaic pattern similar to that of an intervertebral disc

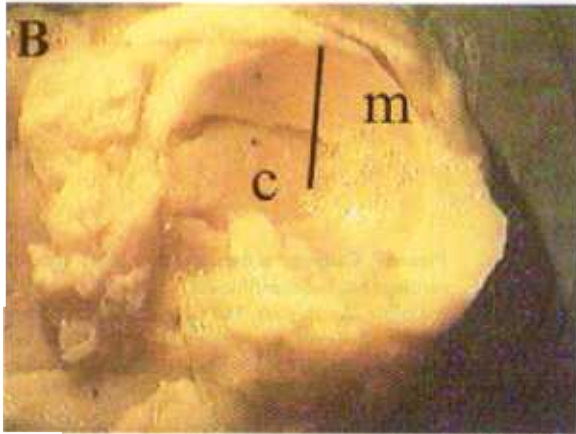
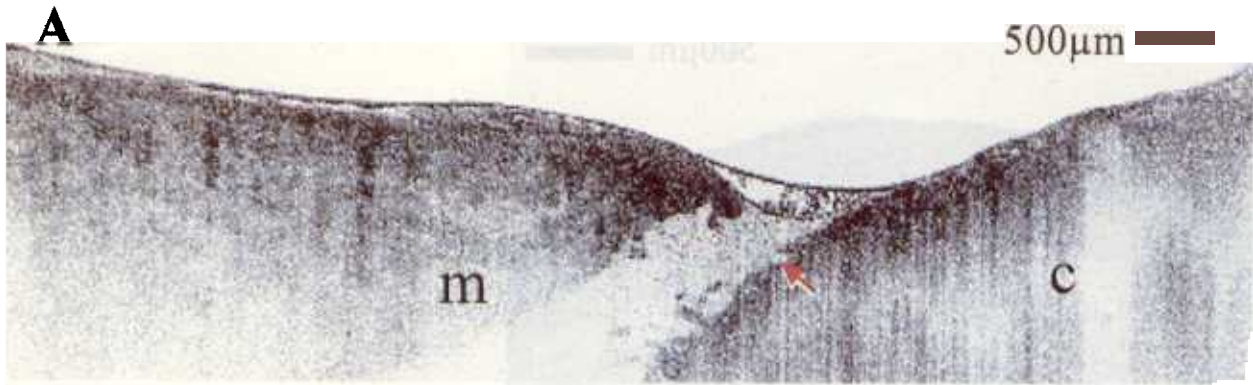


Figure 5. A. OCT image of the medial meniscus (m). The meniscus overlies the articular surface cartilage (c) of tibia (Δz 5 μm). Red arrow shows fibrillations visible in the cartilage through the meniscus. B. A photograph of the joint; the imaging plane is delineated.

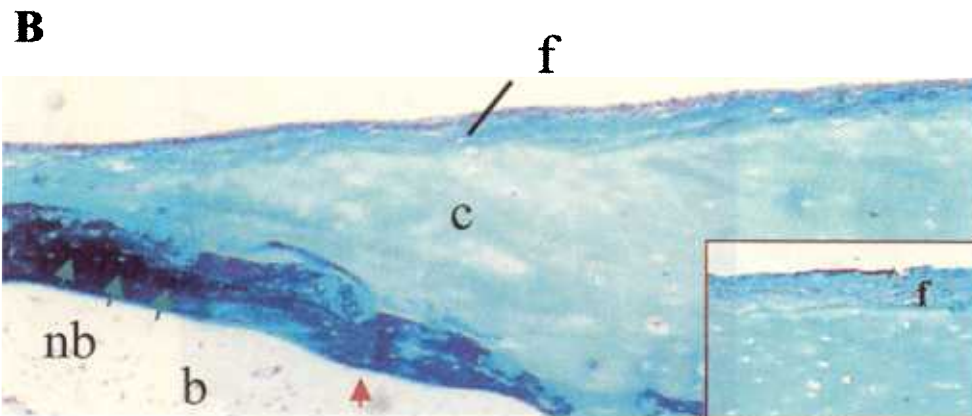
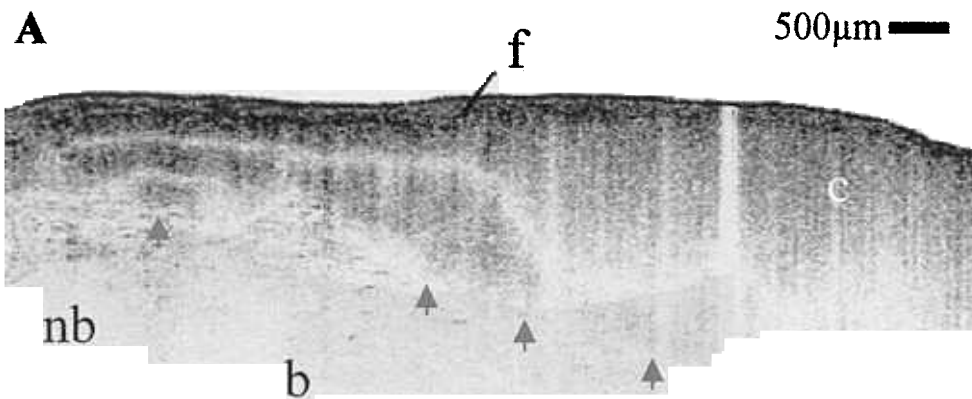


Figure 6. A large and heterogeneous region of bone (b), which represents either irregular subchondral bone or new bone formation. A fibrous layer (f) was resolved at the surface of the cartilage (c). Red arrows show the bone-cartilage interface. The OCT image (A) was confirmed by histology (B) (Δz 5 μm) (trichrome stain). Insert in B is an enlargement of the fibrous layer.

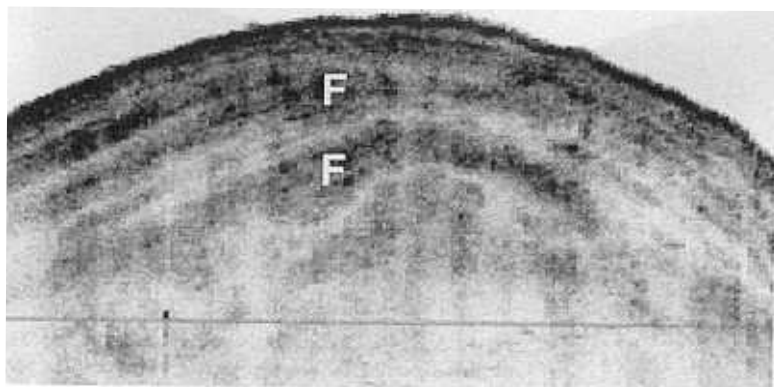

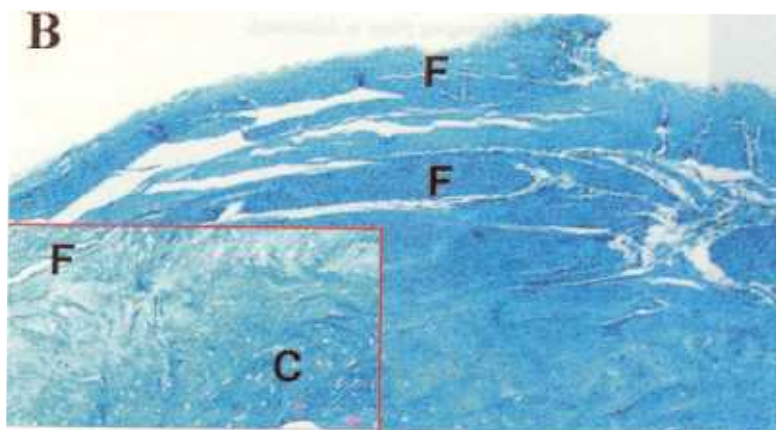
A500 μ m **B**

Figure 7. Cartilage at the clavicular head. The articular cartilage has become fibrocartilage and a mosaic pattern is visible (Δz 16 μ m). The fibrous bands are identified (F). Insert shows enlargement of an interface between cartilage (C) and fibrous tissue (trichrome stain).


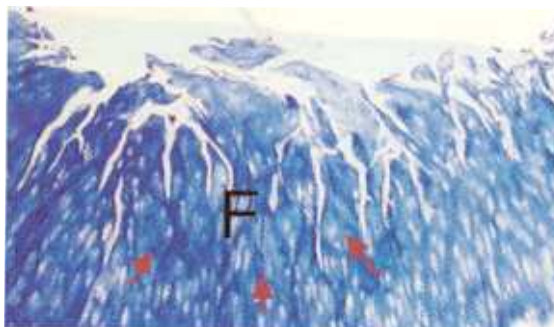
A500 μ m **B**

Figure 8. Fibrillations in cartilage of the knee joint. A. Fibrillation (f) on the surface of the femur in the knee is visible (Δz 5 μ m). The histology of a region nearby is shown in B (trichrome stain).

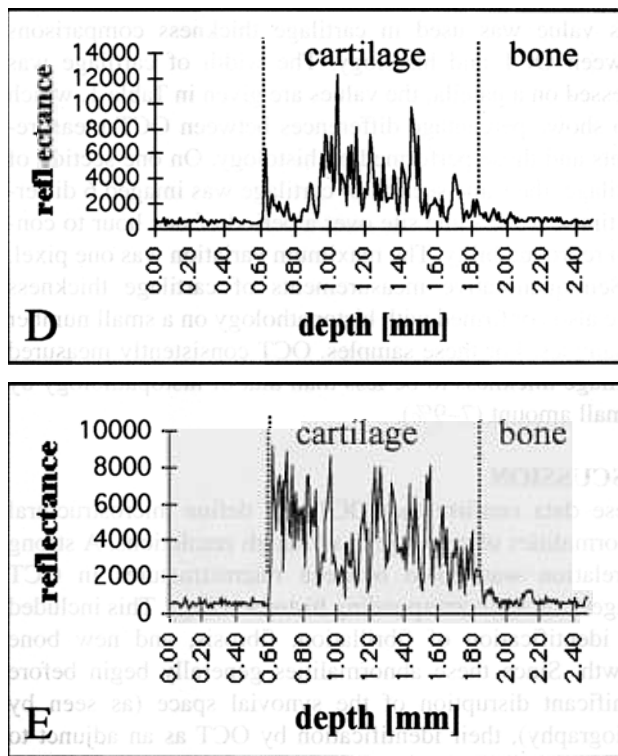
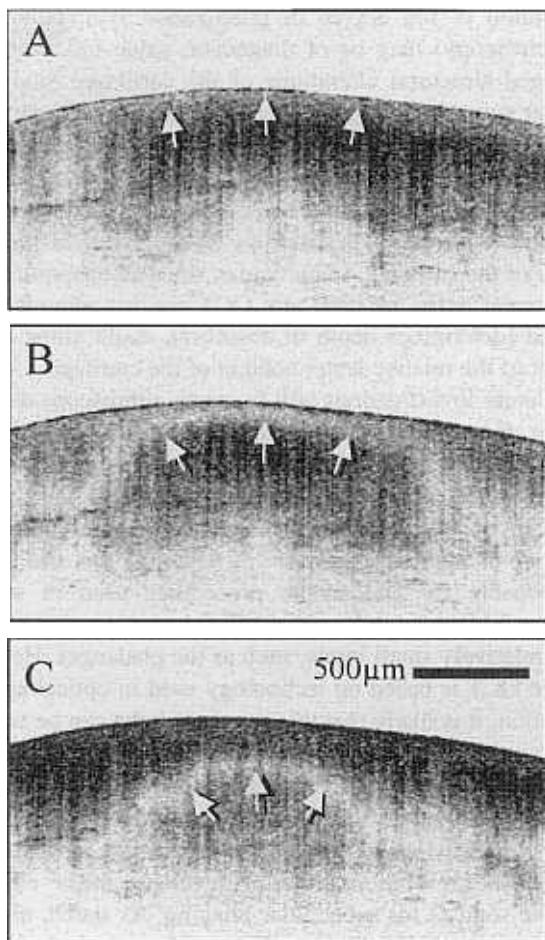


Figure 9. The same area of cartilage of an interphalangeal toe joint is shown with 3 different incident polarization states (A to C) (Δz 15 μm). The measured intensity of backreflection as a function of depth changes with the polarization state. A layered appearance develops (arrows). This likely results from different orientations of the collagen layers, which are birefringent. D and E show the backreflected intensity in a single axial plane (from Figures A to C) quantitatively. The states of incident polarization are different, which results in a different measured intensity as a function of depth. The cartilage-bone interface can be identified by a sudden drop of the reflectance.

was seen (Figure 7). Fibrillations were noted on the surface of the femoral condyle (Figure 8). In all images, backscattering signal intensity decayed as a function of depth, as would be expected from optical theory¹⁹.

The images shown in Figure 9 illustrate the sensitivity of OCT imaging to the polarization state of the incident light, alluded to in Figures 2 and 3. The same area of interphalangeal cartilage was imaged, but with different incident polarization states (Figure 9). It was seen that the intensity of backreflection as a function of depth changed with the polarization state, and a layered appearance developed in the tissue. This is believed to be secondary to the highly organized structure of collagen, which is known to influence polarization. Since change in collagen orientation is one of the earliest changes of OA, assessments of polarization sensitivity may be of diagnostic value independent of 2 dimensional imaging of structural detail. This effect was shown

quantitatively in Figures 9D and 9E, where the backreflecting intensity in a single axial plane is plotted as a function of depth, but once again with the incident light at different states of polarization.

Refractive index measurements were made from 3 joints

Table 1. The ability of OCT to assess cartilage thickness was directly compared with histology. Measurements were made on a single patella at the center and ± 1 mm from the center. At each site, 8 measurements were made 50 μm apart. Data is expressed as the mean \pm SEM. Values in parentheses represent percentage difference between OCT and histology measurements.

	OCT, mm	Histology, mm (%)
Center (n = 8)	1.660 \pm 0.003	1.779 \pm 0.006 (9)
1 mm (n = 8)	1.744 \pm 0.005	1.906 \pm 0.014 (7)
-1 mm (n = 8)	1.705 \pm 0.006	1.860 \pm 0.009 (9)

and were found to be 1.51 ± 0.009 ($n = 18$; mean \pm SEM). This value was used in cartilage thickness comparisons between OCT and histology. The width of cartilage was assessed on a patella; the values are given in Table 1, which also shows percentage differences between OCT measurements and those performed on histology. On one section of cartilage, the same section of cartilage was imaged 6 different times at the same site over a period of one hour to confirm reproducibility. The maximum variation was one pixel.

Semiquantitative measurements of cartilage thickness were also confirmed with histopathology on a small number of samples. For these samples, OCT consistently measured cartilage thickness to be less than that of histopathology by a small amount (7–9%).

DISCUSSION

These data confirm that OCT can define microstructural abnormalities of cartilage at ultrahigh resolutions. A strong correlation was noted between microstructures in OCT images and the corresponding histopathology. This included the identification of fibrillation, fibrosis, and new bone growth. Since these abnormalities generally begin before significant disruption of the synovial space (as seen by radiography), their identification by OCT as an adjunct to therapeutic intervention could help to decrease patient morbidity and progression of the disease.

With regard to the semiquantitative measurements of cartilage thickness, we postulate at least 2 possible explanations for OCT consistently measuring cartilage thickness to be less than that measured by histopathology by 7–9%. First, some tissue distortion occurs during histologic processing, which may make the cartilage appear artificially large. Future high precision measurements of cartilage thickness will be performed using stereomicroscope techniques in conjunction with tissue handling protocols described by other investigators²². Second, since the refractive index was only measured on a small number of samples, the value used may represent an overestimation. Refractive index values must be confirmed in a large number of samples with varying degrees of OA. If a wide variation in refractive index exists, a technique known as focus tracking can be employed *in vivo* for assessing the index on a given joint. It should be recognized that the effectiveness of high resolution determination of cartilage thickness for monitoring the progression of OA needs to be validated with *in vivo* patient studies. Changes in cartilage thickness may be non-uniform, and accurate registration of sites from one interrogation to the next may be difficult.

Imaging of cartilage was also noted to be sensitive to the polarization of incident light. This polarization sensitivity is presumed to be related to the structural organization of the collagen fibers, which is also the basis of polarization microscopy in this tissue²³. Since collagen disorganization is one of the earliest changes in association with OA, quan-

tification of the degree of polarization (i.e., polarization spectroscopy) may be of diagnostic value independent of imaged structural alterations of the cartilage. Studies are under way correlating collagen orientation with polarization sensitivity using polarization microscopy and polarization sensitive staining with picro-sirius red²⁴. In addition to polarization spectroscopy, OCT offers the potential of using infrared absorption spectroscopy for assessing the biochemistry of the cartilage. In particular, since an absorption peak for water exists at 1500 nm, OCT spectroscopy, which is gated (determines depth of absorber), could allow assessment of the relative water content of the cartilage.

Future investigations will focus on arthroscope development, increasing resolution, and extension to *in vivo* imaging. The current OCT imaging endoscope consists primarily of an optical fiber and light directing devices (lens, prism), making it relatively inexpensive. This endoscope is 2.9 French or 1 mm in diameter^{25,26}. Although this size may be reasonable for endoscopic procedures used in surgical suites, it is too large for either office based imaging or imaging relatively small joints, such as the phalanges. However, since OCT is based on technology used in optical communication, it is likely that this imaging probe can be substantially reduced in size. The optical fiber currently used is only 124 μm in diameter, so a system capable of being introduced through a 20 gauge needle remains a possibility.

Future studies will investigate both the advantages of increasing resolution and the development of clinically viable sources for subcellular imaging. As stated, the axial resolution in OCT imaging is dependent on the bandwidth or wavelength distribution of the source. In this study, 3 different bandwidths were used. The system with the lowest resolution, a 1300 nm diode, is compact, stable, and inexpensive. However, it lacks the power necessary for high speed *in vivo* imaging. A solid state laser was also used as a source in this study; in addition to the higher power, it generated resolutions of either 11 or 5 μm , depending on the bandwidth the laser was set to generate. As anticipated, visibility of structural detail was superior at the higher axial resolution. Although the broad bandwidth solid state lasers generate resolutions near the cellular level, with some systems in the range of 3 μm , they are not clinically useful sources due to their complexity¹³. However, compact, inexpensive sources with similar wavelength characteristics are under development that will likely allow cellular level imaging in the clinical setting.

Future *in vitro* and *in vivo* investigations will address many clinically relevant questions that remain, including the ability of OCT to assess other articular structures, joints, and disease processes. Imaging of structures other than the articular cartilage may have important clinical implications for intraarticular imaging. Examples would include examinations of synovium and synovial fluid, although like saline, the latter is expected to be optically transparent unless

severe inflammation or hemoarthrosis is present. In addition, only a few joints were examined in this study to demonstrate feasibility. Imaging needs to be expanded, both *in vitro* and *in vivo*, to all joints where OCT imaging could be of potential use to confirm the initial observations. Finally, other articular disorders, such as chronic inflammatory diseases, need to be examined, since the diagnostic potential of OCT is not limited to OA.

With respect to its ultimate clinical use, broad based routine screening and monitoring of therapy, for most accessible joints, would ideally be performed in an office setting. There are several reasons why office based OCT imaging is a realistic possibility, most of which are a function of its fiber based design. First, as stated, the OCT arthroscope will likely be small and disposable. Second, OCT hardware is compact and portable, roughly the size of a standard personal computer. Finally, the system is relatively inexpensive — the final clinical device will likely be comparable in price to an ultrasound unit.

In conclusion, a need exists for a technology capable of identifying early osteoarthritic changes in cartilage. OCT represents a promising new technology for diagnosing these abnormalities through ultrahigh resolution intraarticular imaging.

ACKNOWLEDGMENT

The authors thank Dr. James Southern, Dr. Guillermo Tearney, Dr. Boris Golubovic, Dr. Scott Martin, and Prof. Gerd Hausler and his group at the University of Erlangen-Nurnberg, Germany, for helpful discussion and comments. Thanks to Cindy Kopf for help in preparation of this manuscript. The assistance of Jeanine Dudac and Jason Corbin in acquisition and handling of tissue is also appreciated.

REFERENCES

1. Itay SA, Abramovici A, Zero Z. Use of cultured embryonal chick epiphyseal chondrocytes as grafts for defects in chick articular cartilage. *Clin Orthop* 1987;220:284-303.
2. Howell DS, Altman RD. Cartilage repair and conservation in osteoarthritis. *Rheum Dis Clin North Am* 1993;19:713-24.
3. Brittberg M, Lindahl A, Nilsson A, Ohlsson C, Isaksson O, Peterson L. Treatment of deep cartilage defects in the knee with autologous chondrocyte transplantation. *New Engl J Med* 1994;331:879-95.
4. Brandt KD. Pathogenesis of osteoarthritis. In: Kelly WN, Harris ED Jr, Ruddy S, Sledge CB, editors. *Textbook of rheumatology*. 3rd edition. Philadelphia: WB Saunders; 1989.
5. Chan WP, Lang P, Stevens MP, et al. Osteoarthritis of the knee: comparison of radiology, CT, and MR imaging to assess extent and severity. *Am J Res* 1991;157:799-806.
6. Myers SL, Dines K, Brandt DA, Brandt KD, Albrecht ME. Experimental assessment by high frequency ultrasound of articular cartilage thickness and osteoarthritic changes. *J Rheumatol* 1995;22:109-16.
7. Adams ME, Wallace CJ. Quantitative imaging of osteoarthritis. *Semin Arthritis Rheum* 1991;20 Suppl 2:26-39.
8. Agemura DH, O'Brien WD, Olerud JE, Chun LE, Eyre DE. Ultrasonic propagation properties of articular cartilage at 100 MHz. *J Acoust Soc Am* 1990;87:1786-91.
9. Ike RW, O'Rourke KS. Detection of intraarticular abnormalities in osteoarthritis of the knee. A pilot study comparing needle arthroscopy with standard arthroscopy. *Arthritis Rheum* 1993;36:1353-63.
10. Tyler JA, Watson PJ, Koh HL, Herrod NJ, Robson M, Hall LD. Detection and monitoring of progressive degeneration of osteoarthritic cartilage by MRI. *Acta Orthop Scand* 1995;66 Suppl 266:130-8.
11. Recht MP, Resnik D. Magnetic resonance imaging of articular cartilage: the state of the art. *J Rheumatol* 1995;22 Suppl 43:52-5.
12. Huang D, Swanson EA, Lin CP, et al. Optical coherence tomography. *Science* 1991;254:1178-81.
13. Bouma BE, Tearney GJ, Boppart SA, Hee MR, Brezinski ME, Fujimoto JG. High resolution optical coherence tomographic imaging using a modelocked Ti:Al₂O₃ laser. *Opt Lett* 1995; 20:1486-8.
14. Puliafito CA, Hee MR, Lin CP, et al. Imaging of macular disease with optical coherence tomography. *Ophthalmology* 1995; 102:217-29.
15. Schmitt J, Yadlowsky M, Bonner R. Subsurface imaging of living skin with optical coherence microscopy. *Dermatology* 1995; 191:93-8.
16. Fujimoto JG, Brezinski ME, Tearney GJ, et al. Optical biopsy and imaging using optical coherence tomography. *Nature Med* 1995;1:970-2.
17. Brezinski ME, Tearney GJ, Bouma BE, et al. Optical coherence tomography for optical biopsy: properties and demonstration of vascular pathology. *Circ* 1996;93:1206-13.
18. Brezinski ME, Tearney GJ, Weissman NJ, et al. Assessing atherosclerotic plaque morphology: comparison of optical coherence tomography and high frequency ultrasound. *Heart* 1997;77:397-403.
19. Schmitt JA, Knuttel M, Yadlowsky J, Eckhaus MA. Optical coherence tomography of a dense tissue: statistics of attenuation and backscattering. *Phys Med Biol* 1994;39:1705-20.
20. Fujimoto JG, Boppart SA, Tearney GJ, Bouma BE, Pitris C, Brezinski ME. High resolution *in vivo* intraarterial imaging with optical coherence tomography. *Heart* 1999; (in press).
21. Tearney GJ, Brezinski ME, Bouma B, et al. Determination of the refractive index of highly scattering human tissue using optical coherence tomography. *Opt Lett* 1995;20:2258-60.
22. Jurvelin JS, Rasanen T, Kolmonen P, Lyyra T. Comparison of optical, needle probe, and ultrasonic techniques for the measurement of articular cartilage thickness. *J Biomechanics* 1995;28:231-5.
23. Speer DP, Dahners L. The collagenous architecture of articular cartilage. *Clin Orthop Rel Res* 1979;139:267-75.
24. Junqueira LC, Bignolas G, Brentani RR. Picrosirius staining plus polarization microscopy, a specific method for collagen detection in tissue sections. *Histochem J* 1979;11:447-55.
25. Tearney GJ, Boppart SA, Bouma BE, et al. Scanning single-mode fiber optic catheter-endoscope for optical coherence tomography. *Opt Lett* 1996;21:543-5.
26. Tearney GJ, Brezinski ME, Bouma BE, et al. *In vivo* endoscopic optical biopsy with optical coherence tomography. *Science* 1997;276:2037-9.